Pulmonary Circulation
Open Access

PVRI | WILEY

Bleomycin-induced lung injury: Revisiting an old tool to model group III PH associated with pulmonary fibrosis

Diana Santos-Ribeiro[1] ⓘ | Marylène Lecocq[1] | Michele de Beukelaer[2] | Caroline Bouzin[2] | Mihaly Palmai-Pallag[3] | Yousef Yakoub[3] | François Huaux[3] | Sandrine Horman[4] | Frederic Perros[5] | Charles Pilette[1,6] | Laurent Godinas[7]

[1]Pneumology, ENT and Dermatology, Institute of Experimental and Clinical Research (IREC), Université catholique de Louvain (UCL), Brussels, Belgium

[2]Imaging Platform (2IP), Institute of Experimental and Clinical Research (IREC), Université catholique de Louvain (UCL), Brussels, Belgium

[3]Institute of Experimental and Clinical Research (IREC), Louvain Center for Toxicology and Applied Pharmacology, Université catholique de Louvain (UCL), Brussels, Belgium

[4]Institute of Experimental and Clinical Research (IREC), Cardiovascular Research Unit, Université catholique de Louvain (UCL), Brussels, Belgium

[5]Laboratoire CarMeN, UMR INSERM U1060/INRA U1397, Université Claude Bernard Lyon1, Pierre-Bénite and Bron, France

[6]Departmen of Pneumology, Cliniques Universitaires St-Luc, Brussels, Belgium

[7]Clinical Department of Respiratory Diseases, University Hospitals and Laboratory of Respiratory Diseases & ThoracicSurgery (BREATHE), Department of Chronic Diseases & Metabolism (CHROMETA), KU Leuven—University of Leuven, Leuven, Belgium

Correspondence
Charles Pilette, Pneumology, ENT and Dermatology, Institute of Experimental and Clinical Research (IREC), Ave Hippocrate 54 Bte B1.54.04 Bernard +3, Brussels 1200, Belgium.
Email: charles.pilette@uclouvain.be

Abstract

Pulmonary hypertension (PH) is a chronic disorder of the pulmonary circulation that often associates with other respiratory diseases (i.e., group III PH), leading to worsened symptoms and prognosis, notably when combined with interstitial lung diseases such as pulmonary fibrosis (PF). PH may lead to right ventricular (RV) failure, which accounts for a substantial part of the mortality in chronic lung disease patients. The disappointing results of pulmonary arterial hypertension (PAH)-related therapies in patients with PF emphasize the need to better understand the pathophysiologic mechanisms that drive PH development and progression in this specific setting. In this work, we validated an animal model of group III PH associated with PF (PH-PF), by using bleomycin (BM) intratracheal instillation and characterizing the nature of induced lung and vascular remodeling, including the influence on RV structure and function. To our knowledge, this is the first work describing this dose of BM in Sprague Dawley rats and the effects upon the heart and lungs, using different techniques such as echocardiography,

---

Charles Pilette and Laurent Godinas contributed equally to this study.

- -

heart catheterization, and histology. Our data shows the successful implementation of a rat model that mimics combined PF-PH, with most features seen in the equivalent human disease, such as lung and arterial remodeling, increased mPAP and RV dysfunction.

KEYWORDS
animal model, cardiovascular diseases, lung remodeling and fibrosis

INTRODUCTION

Pulmonary hypertension (PH) is defined by a mean pulmonary arterial pressure (mPAP) superior to 20 mmHg, measured by right heart catheterization at rest.[1] PH often complicates chronic lung diseases (CLD, referred to as group III PH), contributing to an aggravation of the clinical manifestations and poorer prognosis with increased mortality,[2] especially in pulmonary fibrosis (PF).[3] The disappointing results of clinical trials that assessed the efficacy of PH-specific therapies in patients with PF,[4,5] highlight the need to better understand the mechanisms driving PH development in CLD patients and the identification of new therapeutic targets.

Whereas several animal models of PH[6] and PF[7] have been developed, a validated and well-characterized animal model for group III PH is currently lacking. Bleomycin (BM) is an antibiotic and antitumoral agent produced by *Streptomyces verticillus* that is well known to cause pulmonary toxicity since its first uses as a chemotherapeutic drug,[8] as it may cause severe PF.[9] In the experimental setting, BM was first used to induce PF in dogs,[10] and since then in rats and mice to study the mechanisms and potential therapies of PF.[11] BM induces lung injury through the generation of free radicals that introduce DNA single-strand breaks, causing DNA damage,[12] leading to inflammatory responses and lung tissue fibrosis.[13]

Our aim was to implement and characterize a practical and reproducible animal model mimicking features of combined PF and PH, which could mimic the human group III PH disease associated with PF. In this work, we provide the in-depth characterization of a BM-induced model in rats fully characterized for both pulmonary and vascular remodeling as well as RV remodeling and function.

MATERIALS AND METHODS

Experimental protocol

All animal experiments were performed in agreement with the European Community regulations, followed the recommendations of the *Guide for the Care and Use of Laboratory Animals* (NIH publication No. 85-23, revised 2011) and were approved by the local ethical committee for animal research (2017/UCL/MD/003). Animal handling was performed according to the Federation of European Laboratory Animal Science Association (FELASA). All animals were grouped two or three per cage in a conventional environment with a light-darkness cycle of 12:12 h, controlled temperature and humidity, and water and food ad libitum.

Five- to six-weeks-old male Sprague Dawley rats (Janvier Labs) weighing approximately 250 g were randomly assigned to receive either an intratracheal instillation of 7.5 U/kg of bleomycin sulfate (Sanofi) (BM group, $n = 10–12$) or an equal volume of vehicle (0.9% NaCl) (SL group, $n = 6–8$). Animals were followed by echocardiography (at Days 0, 10, and 20) and at the end of the protocol (Day 21 postinstillation), animals were submitted to an invasive hemodynamic evaluation, followed by euthanasia through exsanguination and sample collection for morphohistological and molecular studies. All tissues measurements were normalized to the length of the tibia (TL).[14]

Echocardiographic evaluation

Echocardiography was performed at baseline, Days 0 (before BM instillation), 10, and 20 in the same conditions. All animals were anesthetized with isoflurane (5% and 2%–3% for induction and maintenance, respectively) (IsoFlo; Zoetis), placed in left lateral decubitus position in a heating pad and the thorax skin was shaved. Echocardiographic evaluation was performed using an MS200 probe (9–18 MHz) and recorded using a Vevo 2100 imaging system (VisualSonics, Fujifilm). Measurements were performed in triplicate and averaged during three consecutive cardiac cycles. Pulmonary artery flow (parasternal long axis) and aortic flow (parasternal short axis) properties were studied, along with the heart rate (HR). In four-chamber view, tricuspid annular

plane systolic excursion (TAPSE) was measured. Cardiac output (CO) was derived from the HR times the stroke volume (SV), which was calculated using the formula: $SV = 7.85 \times AoD^2 \times AoVTI$ (according to VisualSonics Vevo 2100 Imaging System Operator's Manual).

Hemodynamic measurements

At 3-week postinstillation (Day 21) and after anesthesia, animals underwent endotracheal intubation and were connected to a rodent ventilator (RoVent, Kent Scientific Corporation) with an animal weight-defined respiratory rate. Animal's temperature was monitored and regulated by a rectal temperature sensor and a warming pad, respectively. A lower thoracotomy was performed and a pressure catheter (SPR-407; Millar) was inserted through the apex of the RV and LV and positioned along the long axis.[15–19] The experimental preparation was allowed to stabilize for 10–15 min and then recordings were performed. Pressure signals were continuously acquired (Bridge Amp) and digitally recorded at a sampling rate of 1.000 Hz (ML870 PowerLab 8/30; ADInstruments) and analyzed off-line (LabChart 8 Pro; ADInstruments). Baseline hemodynamics parameters were HR, RV, and LV pressures.

Sample collection and morphometric analysis

Immediately after exsanguination, using the endotracheal tube already in place, the lungs were infused two times with 20 ml/kg of chilled 0.9% NaCl. The bronchoalveolar lavage (BAL) was then centrifuged (300g for 5 min at 4°C) and the cell-free supernatant was harvested. The cell pellets of the BAL fractions were resuspended in 1 ml saline to determine cell numbers. Cell differentials were determined on cytocentrifuged preparations stained with Diff-Quick (Baxter). Heart and lungs were excised en bloc. RV free wall, LV plus septum (LV + S), and lungs were dissected and weighed separately. Some lobes of the lungs were collected and snap frozen in liquid nitrogen and stored at −80°C. For histological analysis, samples were directly stored in buffered PFA 4% for 24 h and then included in paraffin blocs. Lung collagen accumulation was estimated by measuring the hydroxyproline (OH-proline) contents by HPLC in lung homogenates as previously described.[20]

Histological analysis and alpha-smooth muscle actin (αSMA) immunohistochemistry

After fixation, histological samples were embedded in paraffin and sections were obtained from RV and lung tissue. For αSMA immunohistochemistry, lung sections were deparaffinized and rehydrated, following an antigen retrieval treatment. Endogenous phosphatases were inactivated and nonspecific protein binding sites were blocked. Sections were incubated overnight with anti-αSMA antibody, washed, and incubated with an alkaline phosphatase-conjugated secondary antibody. Sections were revealed using Fast Red, counterstained with hematoxylin, and coverslipped. Separately, lung sections were also stained with hematoxylin and eosin (HE), Masson's trichrome, and Sirius red, which were used to analyze lung remodeling. Since the injury caused by bleomycin tends to follow a bronchiolocentric pattern, we decided to study separately different areas of the lung, being proximal areas near main bronchi and distal areas near the periphery of the lung, to better understand the pattern assumed in our animal model as well to better detect the changes induced by bleomycin.

Sections were scanned using a digital slide scanner (SCN400; Leica Biosystems) and analyzed using the software TissueIA (SlidePath) and Cytomine open-source software. Sirius red's slides were analyzed under polarized light using an Axioplan microscope (Zeiss), since collagen birefringence changes according to the density of the fibers, which increases with maturation. Immature and thin fibers being weakly birefringent and, therefore, exhibiting a greenish color, and mature and thick fibers being strongly birefringent and displaying a yellow or reddish appearance.[21]

Pulmonary arterial medial wall thickness was calculated as follows: WT % = ((media wall thickness $\times$ 2)/ arterial external diameter) $\times$ 100.

Statistical analysis

Statistical analysis was performed using GraphPad Prism 8 (GraphPad Software Inc.). All graphs are presented as mean $\pm$ SD and differences with $p < 0.05$ were considered statistically significant. Unpaired t-test was used to compare two groups with normal distribution and Welch's correction added in cases where groups had different variances. The Mann–Whitney test was used to compare two groups with non-normal distribution. One-way analysis of variance (ANOVA) with Tukey post-hoc test was used to compare three groups. Two-way ANOVA

Pulmonary Circulation

was used to compare the effect of two different variables between two groups and repeated measures were used to compare two groups along different time points.

RESULTS

Effect of bleomycin instillation on rat weight

It was observed that during the first 7 days post-BM instillation, the rats lost weight (BM vs. SL: -36 ± 24 vs. 73 ± 8 g, $p < 0.0001$). After the first week, their BW began to slowly increase during the course of the experimental protocol (BW gain: 2nd week: 20 ± 32 g, mean $\pm$ SD, vs. 56 ± 11 g, $p < 0.0001$ and 3rd week: 29 ± 22 vs. 43 ± 13 g, $p < 0.0001$), yet never reaching the BW of the SL animals (Figure 1). Contrarily to males, females do not lose weight upon BM instillation (Supporting Information: Figure 2F). No mortality was observed.

Bleomycin induces functional and structural right ventricular alterations

Animals were followed by noninvasive echocardiography. At 3 weeks post-BM challenge, animals presented a decreased pulmonary artery acceleration time (PAAT, Day 20, BM vs. SL: 26.11 ± 2.95 vs. 31.73 ± 2.71 ms $p = 0.0193$) (Figure 2a) and a decreased TAPSE (Day 20, 2.372 ± 0.371 vs. 3.190 ± 0.336 mm, $p = 0.0076$), (Figure 2b,e). RVOT Doppler signal had an altered pattern in animals submitted to BM, characterized by an early systolic peak followed by a slow deceleration time, with the presence of mid-systolic notching (Figure 2d), that highly correlates with the degree of PH and severity.[22] No significant difference was observed in the CO, but a slight decrease (CO, Day 20, 113.5 ± 22.4 vs. 135.1 ± 22.0 ml/min, $p = 0.3749$) (Figure 2c). BM animals had a reduced heart weight when compared to SL animals (0.23 ± 0.03 vs. 0.29 ± 0.01 g/cm, $p < 0.0001$) (Figure 2f), while at the same time, showing a hypertrophied RV as evidenced by Fulton's index (0.50 ± 0.09 vs. 0.29 ± 0.02, $p < 0.0001$) (Figure 2g). Representative histological sections of the heart showed the presence of a thicker RV (Figure 2h). RV cardiomyocytes presented moderate hypertrophy in the BM rats when compared with SL, as showed by the increase in the cardiomyocyte area measured on the cross-sectional area (CSA, 524.8 ± 40.6 vs. 412.9 ± 80.6 μm^2, $p = 0.0205$) in HE-stained RV sections (Figure 2i). No alteration in collagen deposition was observed within the myocardium, as shown by the quantification of stained area on Sirius Red labeled sections (Figure 2j) (BM vs. SL: 17.14 ± 9.38 vs. 22.34 ± 7.77, $p = 0.2404$). Representative samples are illustrated in Figure 2k.
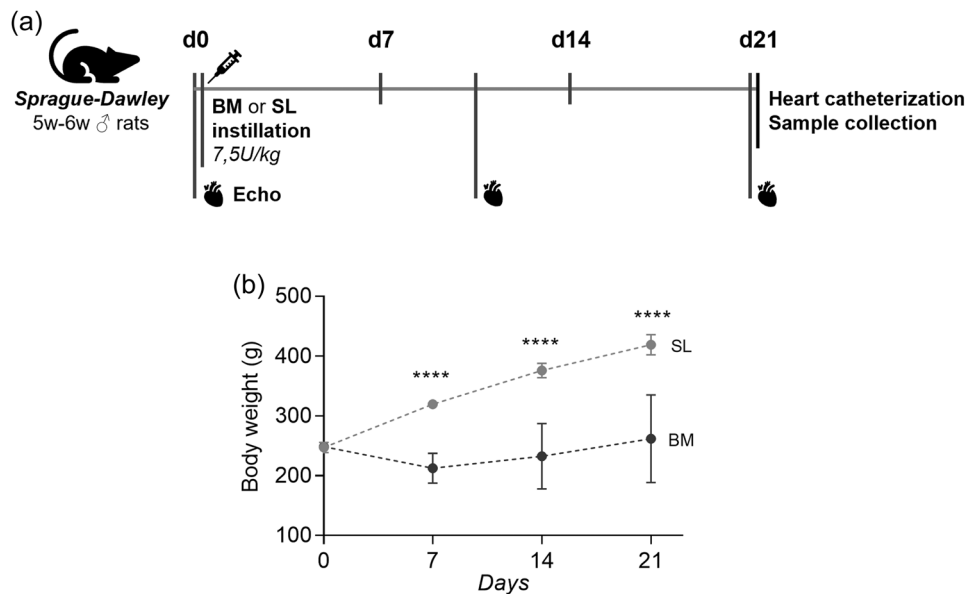
FIGURE 1 Flow chart of the experimental protocol and the effect of bleomycin instillation on rat weight. (a) Flow chart of the experimental protocol. Rats were randomly instilled with either 7.5 U/kg of bleomycin (BM, $n = 10–12$) or equal volume of saline (SL, $n = 6–8$) on Day 0. Rats were submitted to echocardiographic studies at baseline (Day 0), Days 10, and 20 post-BM. Three weeks post-BM (Day 21) rats were subjected to invasive hemodynamic measurements, euthanasia, and sample retrieval. (b) Rat body weight (BW) follow-up since the day of the instillation (Day 0) until the day of sacrifice (Day 21). Symbols indicate mean $\pm$ SD. ****$p < 0.0001$. Unpaired t-test with Welch's correction.
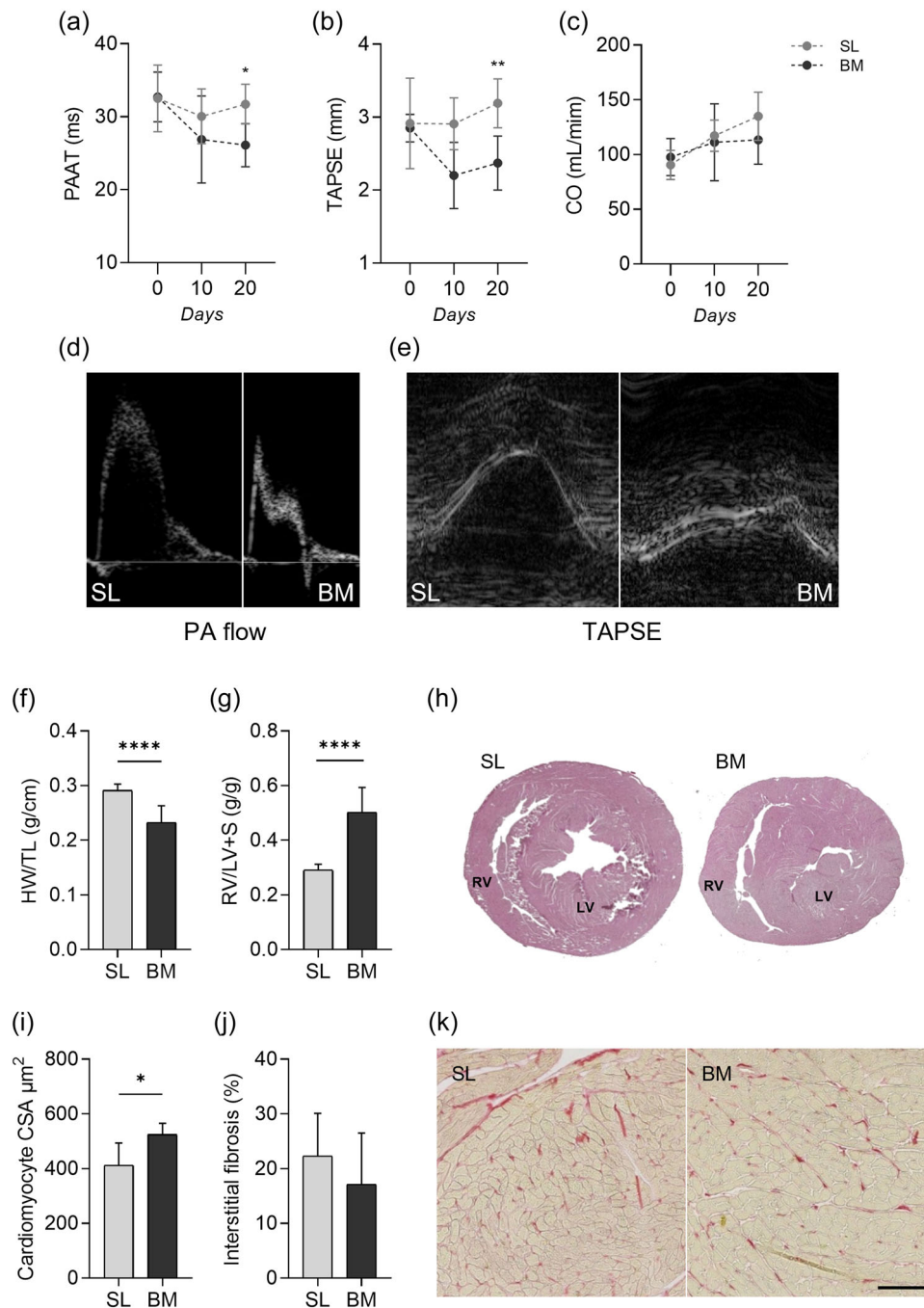
FIGURE 2 Bleomycin induces *cor pulmonale*. (a) Pulmonary artery acceleration time (PAAT) measured by Doppler echocardiography in a long-parasternal axis; (b) tricuspid annular plane systolic excursion (TAPSE) measure by M-mode in a four-chamber view; (c) cardiac output (CO) measured by Doppler in a short-parasternal axis; (d) representative pulmonary arterial flow Doppler signal; (e) representative TAPSE trace; (f) total heart weight normalized for the tibial length (TL); (g) right ventricle (RV) weight normalized to the weight of the left ventricle plus septum (LV + S), also known as Fulton's index, an indicator of right ventricular hypertrophy. (h) Hematoxylin-eosin cross sections of the hearts of SL and bleomycin (BM) animals, showing RV hypertrophy. (i) Cardiomyocyte cross-sectional area quantification; (j) percentage of Sirius red-stained area quantification and (k) representative images of Sirius red-stained RV tissue sections, scale bar = 100 μm. Bars indicate mean ± SD. BM group ($n = 10$–12) and SL group ($n = 6$–8). $*p < 0.05$, $**p < 0.01$, and $****p < 0.0001$ (a–c: Repeated measures two-way analysis of variance with Sidak's post-hoc test; f, g: Unpaired *t*-test with Welch's correction and I, j: Unpaired *t*-test).

Bleomycin induces PH

To confirm the presence of PH in BM-instilled rats, at the end of the experimental protocol, we performed heart catheterization that confirmed the presence of elevated PA pressures (Figure 3a), as showed by the increase in the mPAP (BM vs. SL: 22.5 ± 2.0 vs. 18.5 ± 1.5 mmHg, $p = 0.0002$) (Figure 3b), RVSP (37.5 ± 4.7 vs. 27.3 ± 2.3 mmHg, $p < 0.0001$) (Figure 3c), and TPR (0.34 ± 0.10 vs. 0.16 ± 0.04 mmHg/ml min^{-1}, $p < 0.0044$) (Figure 3d). In addition, a mild decrease in left ventricular systolic pressure (LVSP, 94.9 ± 6.4 vs. 102.5 ± 5.6 mmHg, $p = 0.0149$) was noticed (Figure 3e).

Morphometry and histological assessment

Upon sacrifice, BM rats had heavier lungs when compared with SL rats (BM vs. SL: 1.056 ± 0.1244 vs 0.7989 ± 0.0658 g/cm, $p = 0.0003$) (Figure 4a). Increased collagen deposition was observed with an increase in hydroxyproline (OH-proline) in the lungs of BM rats (784.2 ± 195.2 vs. 624.9 ± 79.5 µg/lung weight, $p = 0.0226$) (Figure 4b). The presence of fibrosis was confirmed by increased Sirius red staining of collagen in both proximal ($23.17 \pm 2.79\%$ vs. $19.17 \pm 4.17\%$, $p = 0.0269$) and distal ($24.67 \pm 4.46\%$ vs. $12.50 \pm 2.43\%$, $p < 0.0001$) areas of the lung (Figure 4c,d). The same lung sections under polarized light were analyzed, and upon quantification a
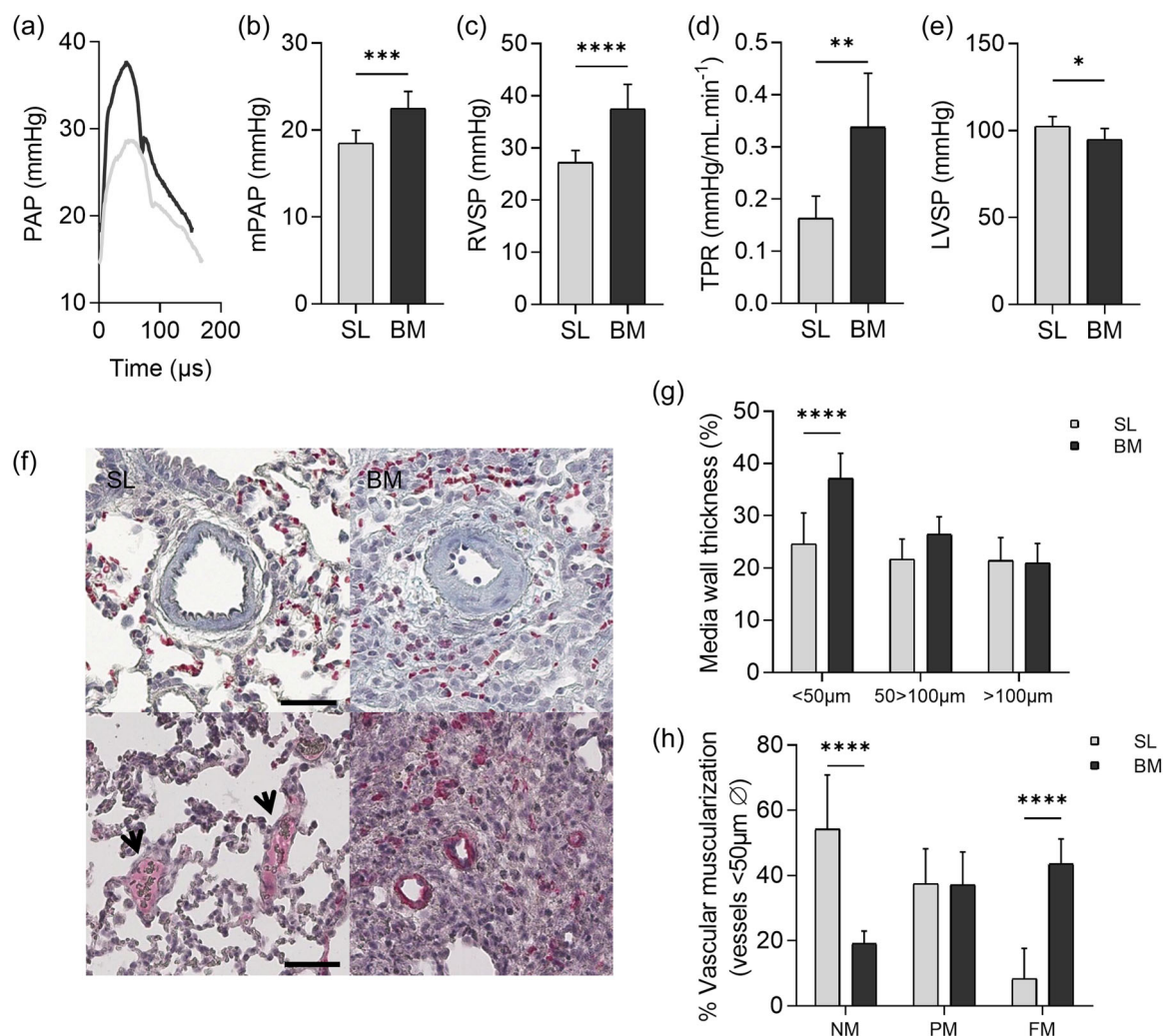
FIGURE 3 Bleomycin induces pulmonary hypertension. (a) Representative pulmonary arterial pressure (PAP) signal; (b) mean PAP, (c) right ventricular systolic pressure (RVSP), (d) total pulmonary resistance (TPR), and (e) left ventricular systolic pressure (LVSP). (f) Representative images of Masson's Trichrome (upper row, scale bar = 25 µ(m) and alpha-smooth muscle actin (αSMA) immunohistochemistry (lower row, scale bar = 50 µm), with the arrows indicating nonmuscularized microvessels; (g) media wall thickness percentage across different vessel caliber; (h) quantification of the percentage of nonmuscularized (NM), partial muscularized (PM), and fully muscularized (FM) microvessels. Symbols/bars indicate mean ± SD. BM group ($n = 10$–12) and SL group ($n = 6$–8). *$p < 0.05$; **$p < 0.001$; ***$p < 0.001$; and ****$p < 0.0001$ (b–e: Unpaired t-test and g, h: two-way analysis of variance).

significant increase in green-colored (but not yellow/red) fibers was observed both proximally ($3.91 \times 10^5 \pm 1.39 \times 10^5$ A.U. vs. $2.03 \times 10^5 \pm 4.59 \times 10^4$ A.U., $p = 0.0039$) and distally ($3.48 \times 10^5 \pm 1.72 \times 10^5$ A.U. vs $1.49 \times 10^5 \pm 7.70 \times 10^4$ A.U., $p < 0.0001$), consistent with early fibrosis with looser fibers (Figure 4e,f). The cross-sectional imaging of the lungs revealed heterogeneity, with patchy areas of fibrosis alternating with areas of normal lung.

Lung sections were further analyzed for vascular remodeling in the BM rats. In Masson's trichrome stained sections (Figure 3f, top panel) the vascular remodeling was mainly present in small arteries (i.e., with a caliber inferior to 50 μm) from BM rats, as shown by the increase in the media wall thickness percentage ($24.64 \pm 5.89\%$ vs. $37.1 \pm 4.83\%$, $p < 0.0001$) (Figure 3g). αSMA-immunostaining (Figure 3f, lower
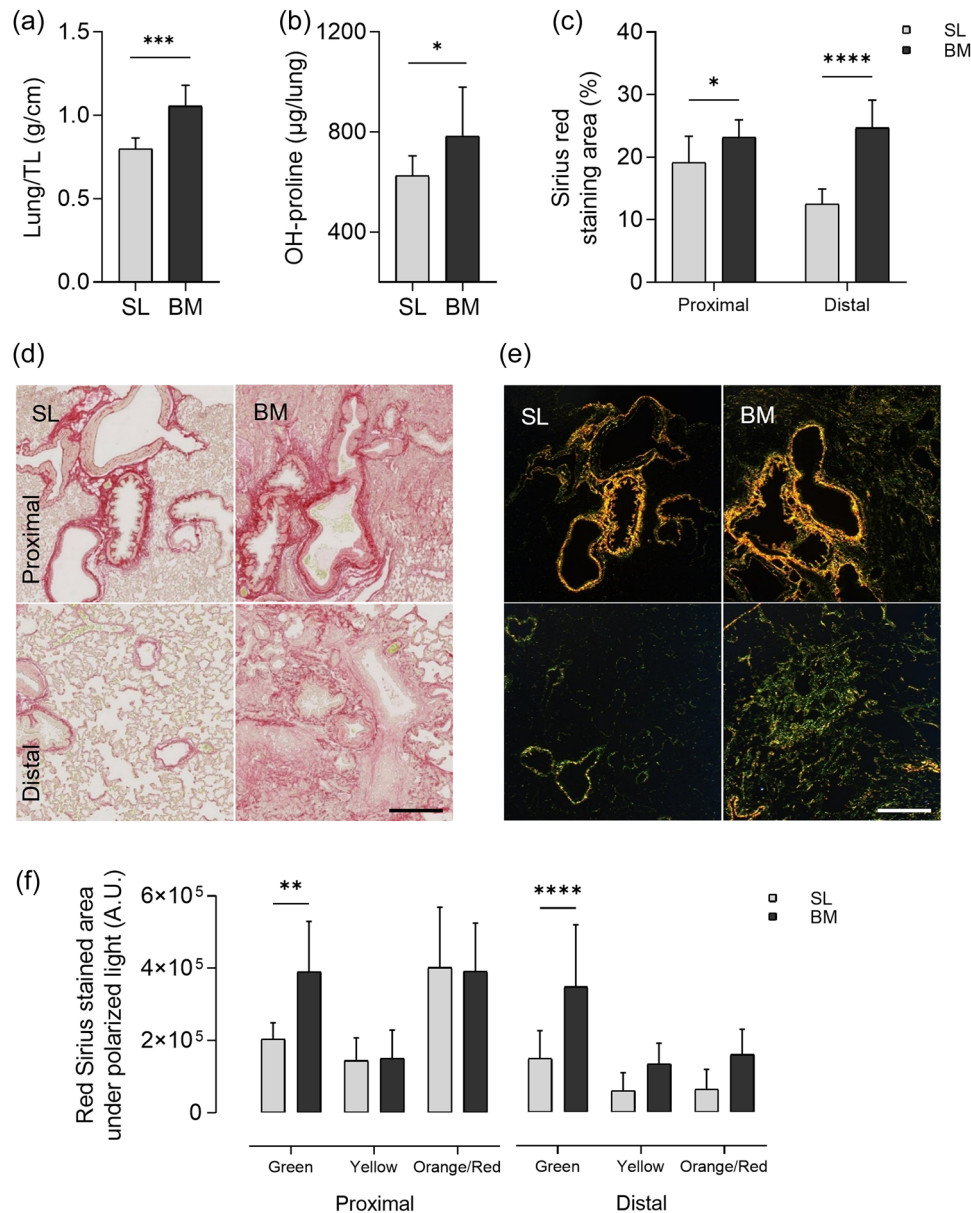
FIGURE 4 Bleomycin induces pulmonary fibrosis. (a) Total lung weight normalized for the tibia's length (TL); (b) hydroxyproline (OH-proline) dosage in right lung lobe tissue homogenates; (c) Sirius red-stained area percentage quantification in proximal and distal areas of the lung; (d) representative images of Sirius red-stained tissue sections of proximal (upper row) and distal (lower row) areas of the lung. Scale bar = 200 μm; (e) representative images of Sirius red-stained tissue sections of proximal (upper row) and distal (lower row) areas of the lung analyzed under polarized light. Scale bar = 200 μm; (f) Sirius red-stained area percentage quantification in proximal and distal areas of the lung, according to the different collagen birefringence, a useful parameter to characterize the maturity of a scar. Bars indicate mean ± SD. BM group ($n = 10–12$) and SL group ($n = 6–8$). *$p < 0.05$; **$p < 0.01$; ***$p < 0.001$; and ****$p < 0.0001$ (a, c: Unpaired t-test; b: Unpaired t-test with Welch's correction and f: two-way analysis of variance).

panel) demonstrated a shift toward a higher percentage of fully muscularized (FM) microvessels ($43.63 \pm 7.59\%$ vs. $8.28 \pm 9.33\%$, $p < 0.0001$) in BM rats, in detriment of nonmuscularized (NM) ($19.19 \pm 3.83\%$ vs. $54.24 \pm 16.65\%$, $p < 0.0001$) (Figure 3h). No significant remodeling was observed in large pulmonary arteries.

BAL analysis and inflammatory response to bleomycin instillation

The presence of inflammation was ascertained by a sixfold increase in total cell numbers in the BAL (SL vs. BM: $1.05 \times 10^7 \pm 7.47 \times 10^6$ vs $1.74 \times 10^6 \pm 1.37 \times 10^6$ cells, $p = 0.0208$) (Figure 5a). This increased cellularity was seen for lymphocytes number ($1.17 \times 10^6 \pm 1.09 \times 10^6$ vs. $1.02 \times 10^5 \pm 1.37 \times 10^5$, $p = 0.0109$) and neutrophils number ($6.80 \times 10^5 \pm 4.92 \times 10^5$ vs. $7.19 \times 10^4 \pm 1.72 \times 10^5$, $p = 0.0062$), as well as a trend for macrophages number ($6.88 \times 10^6 \pm 7.08 \times 10^6$ vs. $1.55 \times 10^6 \pm 1.29 \times 10^6$, $p = 0.0653$), with no change for eosinophils number ($2.81 \times 10^4 \pm 3.87 \times 10^4$ vs. $9.31 \times 10^3 \pm 1.52 \times 10^4$, $p = 0.6084$) (Figure 5b).

DISCUSSION

In this study, we showed that BM instillation resulted in diffuse PF accompanied by microvascular remodeling, leading to RV hypertrophy and dysfunction, recapitulating the three salient features of PH secondary to PF.

Indeed, most of the studies models of group III PH use hypoxemia.[23] Hypoxemia is well known to give perivascular inflammation, pulmonary vascular remodeling, and mild-to-moderate PH.[23] However, there are no significant involvement of the parenchyma, which is a feature encountered in most the CLD, reducing the

possibility to study PH associated with parenchymal remodeling like in PF or emphysema.

Bleomycin is commonly used to model lung injury in rodents and several routes of administration, apart from intratracheal, were already tested, including: Intranasal, subcutaneous, intraperitoneal, and intravenous.[24] The differences between local and systemic routes of BM administration reflect mainly the nonspecific inflammatory response and the magnitude of initial injury.[25]

The use of a single intratracheal instillation, as opposed to other routes of administration or the need for repeated dosing, is easy to implement, less time-consuming, and reproducible.[11] In addition, the local administration of BM decreases the risk of systemic effects and toxicity, while increasing the impact of the drug in the lungs.[25]

To date, several doses of BM using the single intratraqueal method have been described to be able to induce PH in the rat. Prior this protocol, two doses of bleomycin were tested and the presence of PH was investigated (Supporting Information: Figure 1). In contrast to our study, Wistar rats receiving a lower dose of BM develop higher degree of PH, with an RVSP reaching up to ~60 mmHg[26] and an mPAP of ~30 mmHg, with evidence of RV dysfunction.[27,28] This heterogeneity might be in part attributed to the rat strain used in the studies. Wistar rats showing increased susceptibility to pulmonary vascular pathology upon monocrotaline[29] or hypoxia[30] models. In the monocrotaline-induced PH model, Wistar rats injected with 40 mg/kg of monocrotaline reach the same degree of PH and RV hypertrophy as SD rats injected with a higher dose (60 mg/kg).[29] When submitted to chronic hypoxia, Wistar rats develop a more robust polycythemia and RV hypertrophy when compared with SD rats, most likely due to the fact that Wistar rats show increased vascular smooth muscle cytosolic free Ca^{2+} concentration, known to be an important
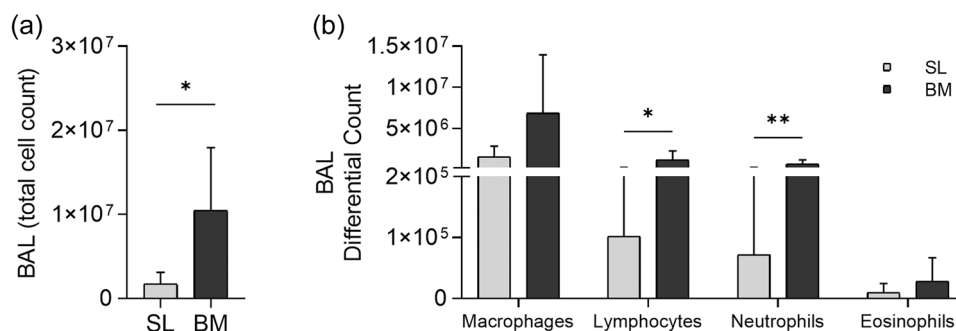
FIGURE 5 Bronchoalveolar lavage (BAL) analysis and inflammatory response to bleomycin instillation. (a) Total cell numbers present in the BAL and (b) differential cell count including macrophages, lymphocytes, neutrophils, and eosinophils present in the BAL. Bars indicate mean $\pm$ SD. Bleomycin group ($n = 10-12$) and SL group ($n = 6-8$). *$p < 0.05$; **$p < 0.01$ (a: Unpaired t-test with Welch's correction and b: Mann–Whitney test).

mediator in vasoconstriction and arterial remodeling.[30] In addition, some variability is also reported even between colonies of the same strain.[31] Variability might also be related with animal gender, however, we did not observe any striking difference between males and females in response to BM in any of the parameters studied, except in BW, which did not decrease upon BM instillation (Supporting Information: Figure 2).

Systemic routes of administration are known to induce rather subpleural extracellular matrix deposition.[32] The lungs of BM-instilled rats showed predominantly bronchiolocentric fibrosis with the presence of sporadic subpleural fibrosis in certain areas, similar to PF in humans. However, to estimate the maturity of the scar, we analyzed the Sirius red-stained slides under polarized light since collagen birefringence changes as the tissue fibrosis matures.[21] The scar observed in the lungs of BM rats exhibited low birefringence and, therefore, displayed a greenish color, meaning that the scar was made up of thin and lightly packed fibers, suggesting an active disease and an early phase of the fibrosis.[33]

One of the main limitations of our work is that we did not study lung/vascular structure and function at other time points besides at the end of the experimental protocol (at Day 21). Therefore, it becomes hard to discriminate either PH advanced purely due to the progressive destruction of lung parenchyma that leads to capillary rarefaction and increased hypoxemia, or if it developed due to endothelial injury triggers by the BM toxicity, already known have this cause-effect.[34] Also, no lung function and/or gas exchange measurements were performed on these animals, hindering the study of a possible correlation between lung destruction and vascular function. In patients, often the degree of PH does not correlate with the severity of the underlying lung disease, indicating that PH might progress independently.[3] A previous study in rats from Jarman et al.,[35] described fibrotic alterations as early as 3 days post-BM instillation, while vascular remodeling and increased pulmonary pressures only showed a meaningful change after 7 and 10 days post-BM, respectively. In accordance, our serial echocardiographic evaluation showed significant alterations in the pulmonary and RV function approximately 20 days post-BM, indicating the development of PH in later stages of the experimental protocol.

Since we noticed some alteration in RV structure/function in rats submitted to BM, it would have been valuable to perform a more in-depth hemodynamic characterization, by using pressure–volume measurements, to remove the effects of load on heart function. In future protocols, it could be interesting to prolong the time of the experimental protocol to study the stability of the parenchymal/vascular lesions, since according to several reports, the bleomycin injury eventually resolves,[36] on the other hand, this dose of BM is one of the highest used in the literature and its stability, to our knowledge, has never been reported. It would be interesting to address if the lung structure repairs, if the alterations in the vasculature and in the RV accompany as well.

CLD are commonly complicated by RV hypertrophy and dysfunction, due to the presence of chronic hypoxemia and vascular remodeling that contribute to increased RV afterload.[37] Similarly, in our animal model, we were able to induce a mild increase in PA pressures along with RV hypertrophy and dysfunction, as observed by the increase in Fulton's index and decrease in TAPSE, while CO was maintained. These specific features resume particularly well the cardiopulmonary phenotype encountered in humans. Indeed, overt right ventricular failure is rare in patients with CLD.[37] The heart of BM-instilled rats was slightly smaller and developed lower pressures when compared with SL. This might be explained due to the ventricular interdependence,[38] since the alterations in the RV directly affect LV function and structure. Moreover, we believe that the slight decrease in the LVSP observed in BM animals when compared to SL, could result from the same insult leading to a lower BW, possibly due to some growth retardation, since the weight of the LV correlated perfectly with the BW, while the RV did not. In addition, no difference was observed in LVEDP (Supporting Information: Figure 3).

Altogether, this study revisited the BM model and reconciled previous studies to implement a novel and simple animal model of combined PF-PH. Our data shows that a single intratracheal dose of BM results in both parenchymal and arterial remodeling consisting of early fibrosis and inducing RV hypertrophy and dysfunction, the three main features observed in group III PH patients. The strength of our work lies in the complete characterization of the fibrotic scarring within the lung and the study of RV and LV function by using echocardiography, invasive hemodynamic evaluation, and histological study of RV myocardium. This enhances the utility of the BM model not only to study lung fibrotic processes but also to study the pathophysiological mechanism leading to the development of PH following fibrosis, allowing for the preclinical testing of candidate drugs.

AUTHOR CONTRIBUTIONS

Diana Santos-Ribeiro performed most of the experiments, analysis, and statistics and drafted the paper. Marylène Lecocq provided the technical know-how and help with tissue processing. Michele de Beukelaer performed conventional histological staining's. Caroline Bouzin provided

the technical know-how and help with the quantification of histological sections. Mihaly Palmai-Pallag and Yousef Yakoub performed preliminary bleomycin experiments to define the correct bleomycin dose and performed HPLC for hydroxyproline. François Huaux shared technical knowledge for the bleomycin model. Sandrine Horman shared all the equipment necessary for the cardiovascular evaluation of the animals; Diana Santos-Ribeiro, Frederic Perros, Laurent Godinas, and Charles Pilette designed the study. Diana Santos-Ribeiro, Laurent Godinas and Charles Pilette reçviewed the data and wrote this manuscript.

CONFLICT OF INTEREST
The authors declare no conflict of interest.

ETHICS STATEMENT
All animal experiments were performed in agreement with the European Community regulations, followed the recommendations of the Guide for the Care and Use of Laboratory Animals (NIH publication No. 85-23, revised 2011) and were approved by the local ethical committee for animal research (2017/UCL/MD/003). Animal handling was performed according to the Federation of European Laboratory Animal Science Association (FELASA).

ORCID
Diana Santos-Ribeiro http://orcid.org/0000-0003-2528-142X

REFERENCES
1. Humbert M, Kovacs G, Hoeper MM, Badagliacca R, Berger RMF, Brida M, Carlsen J, Coats AJS, Escribano-Subias P, Ferrari P, Ferreira DS, Ghofrani HA, Giannakoulas G, Kiely DG, Mayer E, Meszaros G, Nagavci B, Olsson KM, Pepke-Zaba J, Quint JK, Rådegran G, Simonneau G, Sitbon O, Tonia T, Toshner M, Vachiery JL, Vonk Noordegraaf A, Delcroix M, Rosenkranz S. 2022 ESC/ERS guidelines for the diagnosis and treatment of pulmonary hypertension. Eur Respir J. 2022:2200879. In press. https://doi.org/10.1183/13993003.00879-2022
2. Nathan SD, Barbera JA, Gaine SP, Harari S, Martinez FJ, Olschewski H, Olsson KM, Peacock AJ, Pepke-Zaba J, Provencher S, Weissmann N, Seeger W. Pulmonary hypertension in chronic lung disease and hypoxia. Eur Respir J. 2019;53:1801914. https://doi.org/10.1183/13993003.01914-2018
3. Chebib N, Mornex JF, Traclet J, Philit F, Khouatra C, Zeghmar S, Turquier S, Cottin V. Pulmonary hypertension in chronic lung diseases: comparison to other pulmonary hypertension groups. Pulm Circ. 2018;8:1–10. https://doi.org/10.1177/2045894018775056
4. Nathan SD, Behr J, Collard HR, Cottin V, Hoeper MM, Martinez FJ, Corte TJ, Keogh AM, Leuchte H, Mogulkoc N, Ulrich S, Wuyts WA, Yao Z, Boateng F, Wells AU. Riociguat for idiopathic interstitial pneumonia-associated pulmonary hypertension (RISE-IIP): a randomised, placebo-controlled phase 2b study. Lancet Respir Med. 2019;7:780–90. https://doi.org/10.1016/S2213-2600(19)30250-4
5. Raghu G, Behr J, Brown KK, Egan JJ, Kawut SM, Flaherty KR, Martinez FJ, Nathan SD, Wells AU, Collard HR, Costabel U, Richeldi L, deAndrade J, Khalil N, Morrison LD, Lederer DJ, Shao L, Li X, Pedersen PS, Montgomery AB, Chien JW, O'Riordan TG, ARTEMIS-IPF Investigators. Treatment of idiopathic pulmonary fibrosis with ambrisentan: a parallel, randomized trial. Ann Intern Med. 2013;158:641–9. https://doi.org/10.7326/0003-4819-158-9-201305070-00003
6. Michael E. Yeager KLC. Animal models of pulmonary hypertension: matching disease mechanisms to etiology of the human disease. J Pulm Respir Med. 2014;4:198. https://doi.org/10.4172/2161-105X.1000198
7. B. Moore B, Lawson WE, Oury TD, Oury TD, Sisson TH, Raghavendran K, Hogaboam CM. Animal models of fibrotic lung disease. Am J Respir Cell Mol Biol. 2013;49:167–79. https://doi.org/10.1165/rcmb.2013-0094TR
8. Blum RH, Carter SK, Agre K. A clinical review of bleomycin—a new antineoplastic agent. Cancer. 1973;31:903–14. https://doi.org/10.1002/1097-0142(197304)31:4<903::aid-cncr2820310422>3.0.co;2-n
9. Jones AW. Bleomycin lung damage: the pathology and nature of the lesion. Br J Dis Chest. 1978;72:321–6.
10. Fleischman RW, Baker JR, Thompson GR, Schaeppi UH, Illievski VR, Cooney DA, Davis RD. Bleomycin-induced interstitial pneumonia in dogs. Thorax. 1971;26:675–82. https://doi.org/10.1136/thx.26.6.675
11. Moeller A, Ask K, Warburton D, Gauldie J, Kolb M. The bleomycin animal model: a useful tool to investigate treatment options for idiopathic pulmonary fibrosis. Int J Biochem Cell Biol. 2008;40:362–82. https://doi.org/10.1016/j.biocel.2007.08.011
12. Dorr RT. Bleomycin pharmacology: mechanism of action and resistance, and clinical pharmacokinetics. Semin Oncol. 1992;19:3–8.
13. Kim SN, Lee JS, Yang HS, Cho JW, Kwon SJ, Kim YB, Her JD, Cho KH, Song CW, Lee KH. Dose-response effects of bleomycin on inflammation and pulmonary fibrosis in mice.

Toxicol Res. 2010;26:217–22. https://doi.org/10.5487/TR.2010.26.3.217

14. Greenman AC, Albrecht DM, Halberg RB, Diffee GM. Sex differences in skeletal muscle alterations in a model of colorectal cancer. Physiol Rep. 2020;8:e14391. https://doi.org/10.14814/phy2.14391

15. Pacher P, Nagayama T, Mukhopadhyay P, Bátkai S, Kass DA. Measurement of cardiac function using pressure-volume conductance catheter technique in mice and rats. Nat Protoc. 2008;3:1422–34. https://doi.org/10.1038/nprot.2008.138

16. Adão R, Mendes-Ferreira P, Santos-Ribeiro D, Maia-Rocha C, Pimentel LD, Monteiro-Pinto C, Mulvaney EP, Reid HM, Kinsella BT, Potus F, Breuils-Bonnet S, Rademaker MT, Provencher S, Bonnet S, Leite-Moreira AF, Brás-Silva C. Urocortin-2 improves right ventricular function and attenuates pulmonary arterial hypertension. Cardiovasc Res. 2018;114:1165–77. https://doi.org/10.1093/cvr/cvy076

17. Mendes-Ferreira P, Maia-Rocha C, Adão R, Mendes MJ, Santos-Ribeiro D, Alves BS, Cerqueira RJ, Castro-Chaves P, Lourenço AP, De Keulenaer GW, Leite-Moreira AF, Brás-Silva C. Neuregulin-1 improves right ventricular function and attenuates experimental pulmonary arterial hypertension. Cardiovasc Res. 2016;109:44–54. https://doi.org/10.1093/cvr/cvv244.

18. Adão R, Mendes-Ferreira P, Maia-Rocha C, Santos-Ribeiro D, Rodrigues PG, Vidal-Meireles A, Monteiro-Pinto C, Pimentel LD, Falcão-Pires I, De Keulenaer GW, Leite-Moreira AF, Brás-Silva C. Neuregulin-1 attenuates right ventricular diastolic stiffness in experimental pulmonary hypertension. Clin Exp Pharmacol Physiol. 2019;46:255–65. https://doi.org/10.1111/1440-1681.13043

19. Mendes-Ferreira P, Santos-Ribeiro D, Adão R, Maia-Rocha C, Mendes-Ferreira M, Sousa-Mendes C, Leite-Moreira AF, Brás-Silva C. Distinct right ventricle remodeling in response to pressure overload in the rat. Am J Physiol Heart Circ Physiol. 2016;311:H85–95. https://doi.org/10.1152/ajpheart.00089.2016

20. Bondue B, Sherer F, Van Simaeys G, Doumont G, Egrise D, Yakoub Y, Huaux F, Parmentier M, Rorive S, Sauvage S, Lacroix S, Vosters O, De Vuyst P, Goldman S. PET/CT with 18F-FDG- and 18F-FBEM-labeled leukocytes for metabolic activity and leukocyte recruitment monitoring in a mouse model of pulmonary fibrosis. J Nucl Med. 2015;56:127–32. https://doi.org/10.2967/jnumed.114.147421

21. Dayan D, Hiss Y, Hirshberg A, Bubis JJ, Wolman M. Are the polarization colors of picrosirius red-stained collagen determined only by the diameter of the fibers. Histochemistry. 1989;93:27–9. https://doi.org/10.1007/BF00266843

22. Lopez-Candales A, Edelman K. Shape of the right ventricular outflow Doppler envelope and severity of pulmonary hypertension. Eur Heart J Cardiovasc Imaging. 2012;13:309–16. https://doi.org/10.1093/ejechocard/jer235

23. McGetterick M, Peacock A. Group 3 pulmonary hypertension: challenges and opportunities. Glob Cardiol Sci Pract. 2020;2020:e202006. https://doi.org/10.21542/gcsp.2020.6

24. Moore BB, Hogaboam CM. Murine models of pulmonary fibrosis. Am J Physiol Lung Cell Mol Physiol. 2008;294:L152–60. https://doi.org/10.1152/ajplung.00313.2007

25. Lindenschmidt R, Tryka AF, Godfrey GA, Frome EL, Witschi H. Intratracheal versus intravenous administration of bleomycin in mice: acute effects. Toxicol Appl Pharmacol. 1986;85:69–77. https://doi.org/10.1016/0041-008x(86)90388-1

26. Schroll S, Arzt M, Sebah D, Nüchterlein M, Blumberg F, Pfeifer M. Improvement of bleomycin-induced pulmonary hypertension and pulmonary fibrosis by the endothelin receptor antagonist bosentan. Respir Physiol Neurobiol. 2010;170:32–6. https://doi.org/10.1016/j.resp.2009.11.005

27. Iglarz M, Landskroner K, Bauer Y, Vercauteren M, Rey M, Renault B, Studer R, Vezzali E, Freti D, Hadana H, Schläpfer M, Cattaneo C, Bortolamiol C, Weber E, Whitby BR, Delahaye S, Wanner D, Steiner P, Nayler O, Hess P, Clozel M. Comparison of macitentan and bosentan on right ventricular remodeling in a rat model of non-vasoreactive pulmonary hypertension. J Cardiovasc Pharmacol. 2015;66:457–67. https://doi.org/10.1097/FJC.0000000000000296

28. Iglarz M, Bossu A, Wanner D, Bortolamiol C, Rey M, Hess P, Clozel M. Comparison of pharmacological activity of macitentan and bosentan in preclinical models of systemic and pulmonary hypertension. Life Sci. 2014;118:333–9. https://doi.org/10.1016/j.lfs.2014.02.018

29. Mathew R, Altura BT, Altura BM. Strain differences in pulmonary hypertensive response to monocrotaline alkaloid and the beneficial effect of oral magnesium treatment. Magnesium. 1989;8:110–6.

30. Snow JB, Kanagy NL, Walker BR, Resta TC. Rat strain differences in pulmonary artery smooth muscle Ca(2+) entry following chronic hypoxia. Microcirculation. 2009;16:603–14. https://doi.org/10.1080/10739680903114268

31. Jiang B, Deng Y, Suen C, Taha M, Chaudhary KR, Courtman DW, Stewart DJ. Marked strain-specific differences in the SU5416 rat model of severe pulmonary arterial hypertension. Am J Respir Cell Mol Biol. 2016;54:461–8. https://doi.org/10.1165/rcmb.2014-0488OC

32. Chua F, Gauldie J, Laurent GJ. Pulmonary fibrosis: searching for model answers. Am J Respir Cell Mol Biol. 2005;33:9–13. https://doi.org/10.1165/rcmb.2005-0062TR

33. Pickering JG, Boughner DR. Quantitative assessment of the age of fibrotic lesions using polarized light microscopy and digital image analysis. Am J Pathol. 1991;138:1225–31

34. Kato S, Inui N, Hakamata A, Suzuki Y, Enomoto N, Fujisawa T, Nakamura Y, Watanabe H, Suda T. Changes in pulmonary endothelial cell properties during bleomycin-induced pulmonary fibrosis. Respir Res. 2018;19:127. https://doi.org/10.1186/s12931-018-0831-y

35. Jarman ER, Khambata VS, Li YY, Cheung K, Thomas M, Duggan N, Jarai G. A translational preclinical model of interstitial pulmonary fibrosis and pulmonary hypertension: mechanistic pathways driving disease pathophysiology. Physiol Rep. 2014;2:e121332014. https://doi.org/10.14814/phy2.12133

36. Debnath J, Singh H, George R, Satija L, Chawla N, Sarma Y, Vaidya A, Grewal D. Reversible bleomycin toxicity. Med J Armed Forces India. 2010;66:290–1. https://doi.org/10.1016/S0377-1237(10)80071-1

37. Kolb TM, Hassoun PM. Right ventricular dysfunction in chronic lung disease. Cardiol Clin. 2012;30:243–56. https://doi.org/10.1016/j.ccl.2012.03.005

38. Lazar JM, Flores AR, Grandis DJ, Orie JE, Schulman DS. Effects of chronic right ventricular pressure overload on left ventricular diastolic function. Am J Cardiol. 1993;72:1179–82. https://doi.org/10.1016/0002-9149(93)90990-t

SUPPORTING INFORMATION

Additional supporting information can be found online in the Supporting Information section at the end of this article.

How to cite this article: Santos-Ribeiro D, Lecocq M, Beukelaer Md, Bouzin C, Palmai-Pallag M, Yakoub Y, Huaux F, Horman S, Perros F, Pilette C, Godinas L. Bleomycin-induced lung injury: revisiting an old tool to model group III PH associated with pulmonary fibrosis. Pulm Circ. 2023;13:e12177. https://doi.org/10.1002/pul2.12177